IMPLEMENTATION OF A NOVEL MPPT WITH SINGLE SENSOR FOR SOLAR PV SYSTEM USING A LUO CONVERTER

Sundharajan VENKATESAN[1]
Dept. of Electrical and Electronics Engineering,
Alagappa Chettiar College of Engg.&Tech, Karaikudi-630003, Tamil nadu, India.
venkateee10@gmail.com

Manimaran SARAVANAN[2]
Dept. of Electrical and Electronics Engineering,
Thiagarajar College of Engineering,Madurai-625015,Tamil nadu, India.
saravnan7670@gmail.com

Abstract:*This paper presents performance analysis of novel simplified single sensor based (SSB) maximum power point tracking (MPPT) algorithm for stand-alone photovoltaic(PV) system using DC-DC LUO converter. It is important to simplify the tracking algorithm with cost-effectiveness, at the same time which is able to transfer the maximum power to the load with reduced ripple content for enhancing the performance of the PV system,. The proposed MPPT technique tracks the peak power point using only voltage sensor and it obviates a proportional–integral controller in the control loop. It is thus realized with low cost and reduce the complexity to implement the control algorithm. The high performance DC-DC LUO converter is used in this proposed PV system. The inherent input filtering properties of the LUO converter further reduces the ripple content on load side. This algorithm is compared with existing Perturb and Observe (P&O) algorithm and implemented on a FPGA based platform. The experimental results shows that the proposed MPPT algorithm provides a good tracking capability, high efficiency and also significantly reduces the ripple content .*

Key words: *DC-DC LUO converter, Maximum Power Point Tracking (MPPT), Single Sensor Based (SSB) control, Perturb and Observe (P&O).*

1.Introduction

Literature reports, voluminous research to improve the photovoltaic(PV) power efficiency through material development, development of efficient maximum power point tracking (MPPT) algorithm and use of high performance DC-DC power converter topologies[1]. Today's material technology assures only low to medium energy conversion efficiency PV cell and it does not give much improvement in efficiency.Hence, it is essential to develop efficient maximum power point tracking algorithm and choose high performance DC-DC converter for particular application [2].The problem of using PV power includes fluctuating power output from the PV panel due to unpredictable weather conditions. Results in tapping less than optimum value of power from the PV panel. In addition to this, the presently used DC-DC converters in PV power systems gives high ripple content in the voltage and current. To overcome these issues, varieties of MPPT algorithms such as Perturbation and Observation (P&O), incremental conductance (IncCond) method, fuzzy logic, neural network methods have been proposed in the literature [3]-[8]. The inherent characteristics of each method make them suitable for specific application. Many researchers discussed a comparative study of different MPPT methods in terms of operating conditions, number of sensors, convergence speed, and system cost [9] and the effect of power converter induced voltage and current ripple in PV power system [10],[11]. The ripple effects are often alleviated by adding an filter in the converter side. The addition of filter circuit in the PV system not only increases cost, power losses, and also increases potential failure rate in such converters.

All the existing MPPT methods depend on determination of PV array's power output and/or load power using the instantaneous voltage and current information, require voltage and current sensors. This may not be optimal for small-scale energy generation, because, voltage can be easily measured with a small amount of power using potential divider arrangement. Continuous current measurement using shunt resistor involves significant power loss in the shunt resistor. Hall Effect sensors to measure current are now available but their cost is high. Although most of the MPPT algorithms can closely track and maintain power production at or near MPP, but in that systems efficiency can be considerably improved by limiting the associated losses and power consumption.

The high frequency switching operation of power converter may cause additional voltage and current ripple which impact on the output power loss leads to decrease in over all conversion efficiency. Hence, it is important to observe the input current ripple of the PV energy harvesting system by utilizing efficient power converter topologies [12]. Towards this goal, novel Single Sensor Based (SSB) MPPT algorithm is

implemented and compared with existing P&O algorithm using higher performance DC-DC LUO converter in this proposed work.

This paper is organized as follows. The mathematical model of PV module is given in Section 2. Detailed design of DC-DC LUO converter including state space averaging is discussed in Section 3. Novel SSB MPPT controller is discussed in Section 4. Simulation result analysis of existing P&O and proposed SSB MPPT algorithm is carried out in Section 5. An experimental prototype is deigned and verified in Section 6. Conclusion is given in Section 7.

2.Mathematical Model of PV Panel

A solar cell alters energy in the photons of sunlight into electricity by means of the photoelectric phenomenon. It is modelled by a current source, a diode and two resistors called single diode model of the PV cell. The single diode equivalent circuit model of a PV cell is shown in Fig.1. The diode is connected in parallel to current source; the photon energy incident on the PV cell generates current. The current source (I_{ph}) is proportional to the amount of energy incident on PV cell [13],[14].

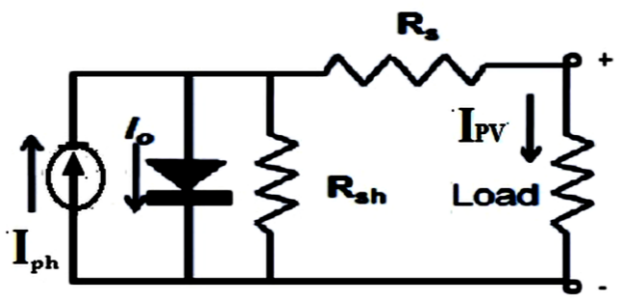

Fig.1. Single diode equivalent circuit model of PV cell

The I-V characteristics of the PV cell model are obtained by the equation [1-3]. The PV cell light generated current I_{ph} depends on the solar irradiation and temperature is given by equation (1)

$$I_{ph} = G_k[I_{sc} + K_i(T_{op} - T_{ref})] \quad (1)$$

The PV module reverse saturation current is given by equation(2)

$$I_{rs} = I_{sc} \Big/ e^{(V_{oc}q/N_sKAT_{op})-1} \quad (2)$$

The module diode saturation current I_o varies with the cell temperature which is given by equation (3)

$$I_o = I_{rs}[\frac{T_{op}}{T_{ref}}]^3 \exp[\frac{q * E_{go}}{BK}\{\frac{1}{T_{ref}} - \frac{1}{T_{op}}\}] \quad (3)$$

The solar cell output current is given by equation (4)

$$I_{pv} = I_{ph} - I_o - I_{sh} \quad (4)$$

Equation (4) can be modified by substituting equation (1-3) and obtained as

$$I_{pv} = N_P * I_{ph} - N_P I_o[\exp\{q * (V_{pv} + I_{pv}R_s)\} - 1] - (V_{pv} + I_{pv}R_s)/R_{sh} \quad (5)$$

Where

V_{pv} : output voltage of a PV module (V)
I_{pv} :output current of a PV module (A)
I_{ph} :The light generated current in a PV module (A)
G_k :Constant which is equal to μ/1000;
μ :The irradiation(irradiation level) (W/m^2)
I_O :Diode saturation current (A)
q :Electron charge (1.6×10^{-19} C)
K :Boltzmann constant (1.38×10^{-23} J/K)
KI :The short-circuit current temperature co-efficient at I_{SC} is 0.0017A / ^{o}C
A=B :Ideality factor =1.6
T_{op} :Cell operating temperature in ^{0}C
T_{ref} :Cell reference temperature at 25^{0}C
R_s :Solar cell series resistance (Ω)
R_{sh} :Solar cell shunt resistance (Ω)
I_{SC} :The PV module short-circuit current at 25 ^{o}C and 1000W/m^2
Ego :The band gap for silicon = 1.1 ev
Ns :The number of cells connected in series in the module
Np :The number of cells connected in parallel in the module

The PV panel is modeled mathematically as per the equations using MATLAB/SIMULINK as shown in Fig. 2. The PV model takes solar irradiation (μ) in W/m^2 and operating temperature (T_{op}) in Celsius as input.

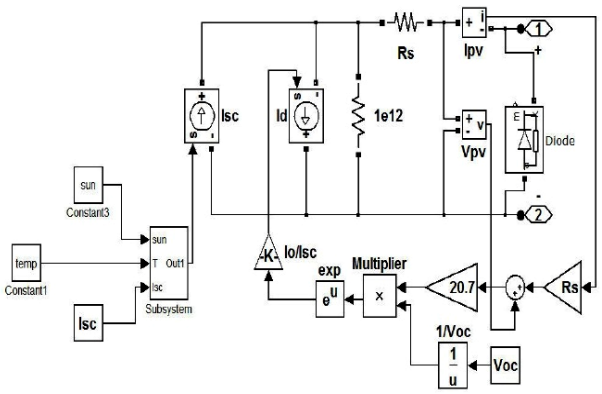

Fig.2 Developed PV panel model in MATLAB

A 40W PV module specification is taken for MATLAB simulation and experimental setup details are given in Table 1. Fig.3 presents the power-voltage (P-V) characteristics of the 40W module under various level of irradiation at a constant temperature of 25^{o}C.

Table 1: Specification of 40W PV panel under STC

Parameter	Value
Rated Power	40W
Short Circuit Current(Isc)	2.45A
Current at Maximum Power(I_{MPP})	2.29A
Voltage at Maximum Power(V_{MPP})	17.3V

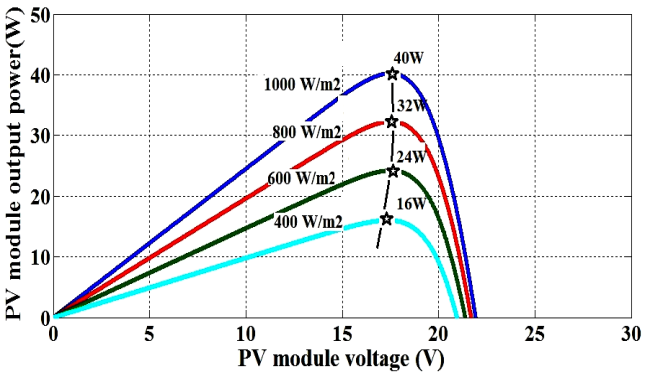

Fig.3 P-V characteristics of 40W solar module under varying weather conditions at 25°C

3. Design of LUO converter

A.Selection of proper converter for PV system

Lot of converters is implemented so far to enhance the performance of PV system. They are differed based on output voltage requirement (buck, boost, buck-boost), output transient, computational performance, voltage and current ripple generation and efficiency etc.[7]. Among all the existing converter topologies, the LUO converter provides a regulated positive output voltage of any required level (higher or lower) from input source voltage, like the buck-boost converter topology. The benefits of LUO converter include lower output voltage ripple, easier compensation and good performance characteristics in particular there is no parasitic problem. Thus, the novel attempt is made using LUO converter in the proposed PV system. Table 2 shows comparison of major characteristic of different DC-DC converters used in PV applications [15]-[17].

Table 2 : Major characteristic of different DC-DC converters

Type	DC-DC Converter	Voltage gain	Output Voltage	Output Transient	R_{eff} from input side of Converter	Computational Performance	Efficiency	
							$R_L<R_{MPP}$	$R_L>R_{MPP}$
Fundamental Converter	Buck	$V_O = D\ V_{in}$	Non-Inverted	High	$R_{in} = \frac{1}{D^2} R_L$	Better	High	Low
	Boost	$V_O = \frac{1}{1-D} V_{in}$	Non-Inverted	High	$R_{in} = (1-D)^2\ R_L$	Not Good	Low	High
	Buck-Boost	$V_0 = \frac{D}{1-D} V_{in}$	Inverted	High	$R_{in} = \frac{(1-D)^2}{D^2} R_L$	Better	High	High
Higher Order Converter	CUK	$V_O = \frac{D}{1-D} V_{in}$	Inverted	Less	$R_{in} = \frac{(1-D)^2}{D^2} R_L$	Average	Medium	High
	SEPIC	$V_O = \frac{D}{1-D} V_{in}$	Non-Inverted	High	$R_{in} = \frac{(1-D)^2}{D^2} R_L$	Average	Medium	High
	LUO	$V_O = \frac{D}{1-D} V_{in}$	Non-Inverted	Less	$R_{in} = \frac{(1-D)^2}{D^2} R_L$	Better	Medium	High

B. LUO converter basic operation

The DC-DC LUO converter is derived from the buck-boost converter. The elementary LUO converter can perform step-up and step-down DC-DC conversion. The basic circuit diagram of the LUO converter as shown in Fig.4 (a). It consists of switch S and D_1 is the diode, capacitor C_1 as the primary means of storing and transferring energy from the input source to the output load via the pump inductor L_1 and a low-pass filter L_2-C_2. and the voltage across the switch is V_S. Choose capacitor C_1 to be large, so that the variation of the capacitor voltage can be neglected [18].

The LUO converter can operate either in Continuous Conduction Mode (CCM) and Discontinuous Conduction Mode (DCM) depending on the current flowing through L_1 . In

this paper CCM mode of operation is considered.

The working principle of LUO converter is analyzed by two modes (ON and OFF state) of the switch condition. The equivalent circuit of this converter when switch S is in ON and OFF condition as shown in Fig.4 (b) & (c). When switch S of the LUO converter is ON mode, the instantaneous source current $i_{in} = i_{L1} + i_{L2}$. Inductor L_1 is absorbs energy from PV source. In the mean time inductor i_{L2} absorbs energy from PV source and capacitor C_1, so both current i_{L1} and i_{L2} increase . When switch S is OFF Mode, source current is zero, current i_{L1} flows through the free-wheeling diode D_1 to capacitor C_1. Inductor L_1 transfers stored energy to capacitor C_1. In the mean time current i_{L2} flows through (C_2 - R) circuit. Both inductor currents $i_{L1}$and i_{L2} decrease. The variations of instantaneous source currents i_{L1} and i_{L2} are small so that $i_{L1} \approx I_{L1}$ and $i_{L2} \approx I_{L2}$. LUO converter inductor and capacitor voltage and current during ON and OFF mode switch is given in Fig. 4.(d).

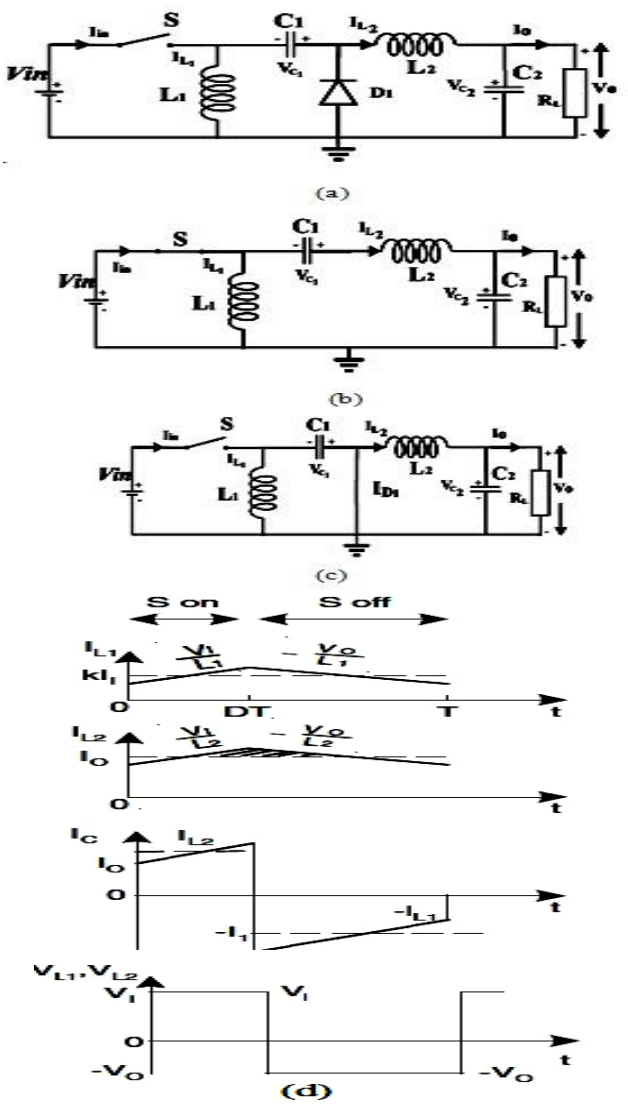

Fig.4. Circuit diagram of (a) LUO converter (b) During Switch ON condition (c) During Switch OFF condition (d) Inductor and capacitor voltage and current waveform of converter circuit

The output voltage expression for LUO converter is given by equation (6),

$$V_o = \frac{D}{1-D} V_{in} \tag{6}$$

where D and V_O is the duty cycle and output voltage of the converter respectively.

C. Design of circuit elements of the LUO converter

The components of the LUO converter used in the simulation and experimental setup are calculated by the following expression,

Selection of Inductors

$$L_1 = \frac{V_{in,min}}{\Delta I_{L_1} \times f_s} \times d_{max}$$

$$L_2 = \frac{V_{in,min}}{\Delta I_{L_2} \times f_s} \times d_{max}$$

Selection of Capacitors

$$\Delta V_{C1} = \frac{I_o \times d_{max}}{C_1 \times f_S}$$

$$\Delta V_{C2} = \frac{d_{max} V_{in\,min}}{8 \Delta C_2 L_2 f_s^2}$$

The LUO converter utilizes the power from the 40-W PV module. Its rated peak power is 40W, rated maximum voltage is 17.3V and rated maximum current is 2.29A. The input voltage (V_{in}) of this converter is approximately 17.4V at 1000W/m^2 and 12.5V at 300 W/m^2 (assuming that the minimum irradiance at the installed location). The desired output (V_o) of the converter should be equal to 36V for typical load resistance of 35 ohm at 1000W/m^2. The specification of the LUO converter is given in Table 3.

Table 3: Specification of LUO converter

Components	Specifications
Source Voltage	12.5V-17.5V
Output Voltage	36V at 1000W/m^2
Inductor, L_1& L_2	200µH & 250µH
Capacitor,C1&C2	25µF & 200µF
Resistive Load, R	35 ohm
Switching frequency(f_s)	25 kHz

D. State Space Model of LUO converter

The state space technique can be used to illustrate the dynamic behavior of a DC-DC LUO converter which yields the average output value with respect to the signal behavior of switching. It is able to handle the system easily with multiple inputs and outputs. The state space model provides a time-domain solution, which is required in this work.The effect of the initial conditions can be easily used into the solution. The matrix modeling is very efficient from a computational standpoint.

The derivation of state equation for the fourth order LUO converter for the ON and OFF state of the switch can be described by the following equations by applying Kirchhoff's laws [19],[20]. The state variables of the LUO converter (x_1, x_2, x_3, and x_4) are considered as inductor currents i_{L_1} and i_{L_2} and capacitor voltages V_{c_1} and V_{c_2} respectively.

During switch ON state, the state space equation for LUO converter written by the equation (7) in terms of state variable,

$$\begin{cases} \dot{X}_1 = \frac{1}{L_1} v_{in} \\ \dot{X}_2 = -\frac{1}{L_2} X_3 - \frac{1}{L_2} X_4 + \frac{1}{L_2} v_{in} \\ \dot{X}_3 = \frac{1}{C_1} X_2 \\ \dot{X}_4 = \frac{1}{C_2} X_2 - \frac{1}{RC_2} X_4 \end{cases} \tag{7}$$

$$\begin{bmatrix} \dot{X}_1 \\ \dot{X}_2 \\ \dot{X}_3 \\ \dot{X}_4 \end{bmatrix} = \begin{bmatrix} 0 & 0 & 0 & 0 \\ 0 & 0 & -\frac{1}{L_2} & -\frac{1}{L_2} \\ 0 & \frac{1}{C_1} & 0 & 0 \\ 0 & \frac{1}{C_2} & 0 & \frac{-1}{RC_2} \end{bmatrix} \begin{bmatrix} i_{L_1} \\ i_{L_2} \\ v_{C_1} \\ v_{C_2} \end{bmatrix} + \begin{bmatrix} \frac{1}{L_1} \\ \frac{1}{L_2} \\ 0 \\ 0 \end{bmatrix} v_{in} \tag{8}$$

During off state, the state equations are written by equation (9)

$$\begin{cases} \dot{X}_1 = -\frac{1}{L_1} X_3 \\ \dot{X}_2 = -\frac{1}{L_2} X_4 \\ \dot{X}_3 = \frac{1}{C_1} X_1 \\ \dot{X}_4 = \frac{1}{C_2} X_2 - \frac{1}{RC_2} X_3 \end{cases} \tag{9}$$

$$\begin{bmatrix} \dot{X}_1 \\ \dot{X}_2 \\ \dot{X}_3 \\ \dot{X}_4 \end{bmatrix} = \begin{bmatrix} 0 & 0 & -\frac{1}{L_1} & 0 \\ 0 & 0 & 0 & -\frac{1}{L_2} \\ \frac{1}{C_1} & 0 & 0 & 0 \\ 0 & \frac{1}{C_2} & 0 & \frac{-1}{RC_2} \end{bmatrix} \begin{bmatrix} X_1 \\ X_2 \\ X_3 \\ X_4 \end{bmatrix} + \begin{bmatrix} 0 \\ 0 \\ 0 \\ 0 \end{bmatrix} v_{in} \tag{10}$$

The state space averaging technique is applied and the resultant state space equation of LUO converter is obtained as (11).

$$\frac{d}{dt} \begin{bmatrix} i_{L_1} \\ i_{L_2} \\ v_{C_1} \\ v_{C_2} \end{bmatrix} = \begin{bmatrix} 0 & 0 & \frac{1}{L_1} & 0 \\ 0 & 0 & 0 & \frac{-1}{L_2} \\ \frac{1}{C_1} & 0 & 0 & 0 \\ 0 & \frac{1}{C_2} & 0 & \frac{-1}{RC_2} \end{bmatrix} \begin{bmatrix} i_{L_1} \\ i_{L_2} \\ v_{C_1} \\ v_{C_2} \end{bmatrix} + \begin{bmatrix} \frac{v_{in} - v_{C_1}}{L_1} \\ \frac{v_{C_1} + v_{in}}{L_2} \\ \frac{-i_{L_1} - i_{L_2}}{C_1} \\ 0 \end{bmatrix} \gamma + \begin{bmatrix} 0 \\ 0 \\ 0 \\ 0 \end{bmatrix} v_{in} \tag{11}$$

$$\dot{X} = AX + B\gamma + C \tag{12}$$

where γ is the status of the switches, and $\dot{X}$ is the derivative of state variables.

$$\gamma = \begin{cases} 1 \rightarrow S \rightarrow ON \\ 0 \rightarrow S \rightarrow OFF \end{cases}$$

4.Maximum Power Point Tracking (MPPT) Algorithm

MPPT is used to adjust the load characteristics under changing irradiation level such that the operating point is always the Maximum Power Point (MPP) corresponding to that irradiation level. Fig.5 shows the PV module interfacing to load and it is well known that the P-V characteristics has only one point where power is maximum, and the corresponding voltage is V_{MPP} and current is I_{MPP}. If load line reaches this point then the maximum power is transferred to the load. The optimum value of resistance PV panel is calculated by PV voltage and PV current at MPP and is given by equation (13).

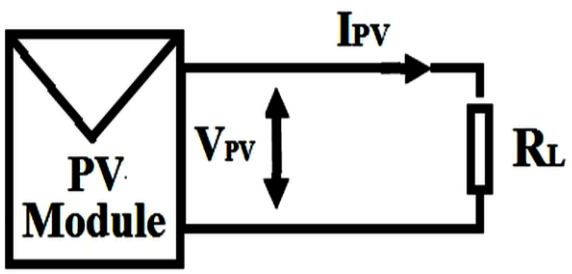

Fig.5 PV module interfacing to Load

$$R_{opt} = \frac{V_{MPP}}{I_{MPP}} \tag{13}$$

where V_{MPP} is the PV voltage at MPP and I_{MPP} is the value of PV current at the MPP.

When the value of load resistance matches with that of R_{opt} maximum power is transfer from PV panel to the load will occur. The objective of the MPPT is to adjust the load resistance to be equal to the source resistance of PV module under change in environmental condition.

A. Proposed SSB MPPT algorithm

PV module exhibits non-linear I-V characteristic. A direct connection of a load to PV array always does not give maximum power to the load. Load line does not intersect with the I-V characteristic of PV source at maximum power point at varying environmental conditions. Hence to operate the PV system at maximum power point, it is required to alter the slope of load line, intersecting the I-V characteristic with the help of converter circuit [21]. In this work, a simplified novel SSB MPPT technique with DC-DC LUO converter is proposed. Generally voltage and current measurement are considered for MPPT implementation but in this proposed work, only voltage measurement is considered as explained in the following section

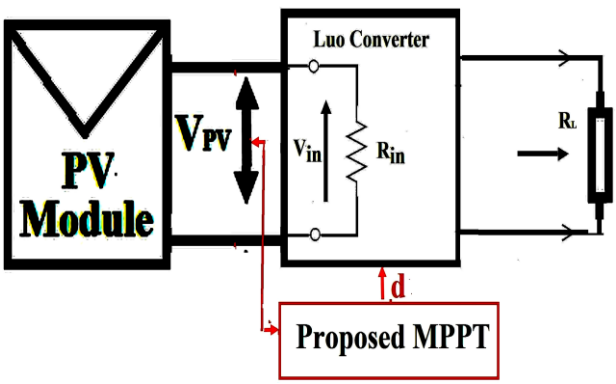

Fig.6 Block diagram of whole system with LUO converter

The reflected input resistance R_{in} of LUO converter with resistive load acts as load for PV module.The R_{in} of LUO converter is given by equation (14). Fig.6 shows the block diagram of the whole system with LUO converter.

By varying the duty cycle, the effective load resistance is adjusted and equal to the internal resistance (R_{opt}) of the solar array at any given irradiation. It is given in equation (14)

$$R_{in} = \frac{V_{in}}{I_{in}} = \left(\frac{1-d}{d}\right)^2 \frac{V_0}{I_0} = \left(\frac{1-d}{d}\right)^2 R_L \qquad (14)$$

The range of R_{in} values for DC-DC LUO converter is shown in Fig.7 for different values of 'd'

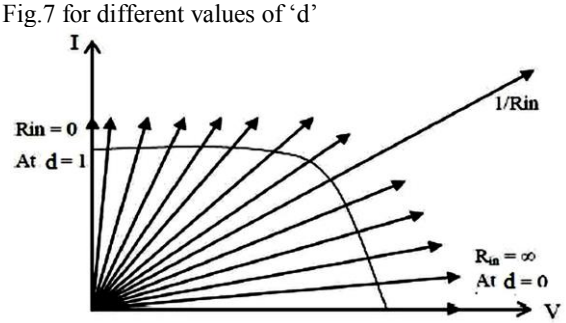

Fig.7 Variation of R_{in} With duty cycle

The PV module power is calculated by the equation as given in (15)

$$P_{pv} = V_{pv} I_{pv} \qquad (15)$$

Equation (15) is written as

$$P_{pv} = V_{pv} \frac{V_{pv}}{R_{in}} \qquad (16)$$

Now R_{in} can be replaced and written as

$$P_{pv} = V_{pv} \frac{V_{pv}}{\left(\left(\frac{1-d}{d}\right)^2 R_L\right)} \qquad (17)$$

In order to derive the maximum power, $\frac{\partial P_{PV}}{\partial d} = \frac{\Delta P_{PV}}{\Delta d} = 0$ for small value of Δd. The duty cycle is continuously adjusted for a fixed step size at regular interval till the ΔP_{PV} reaches zero, a small marginal error of 0.02 was allowed in this work. This process repeats itself until the maximum peak power point is reached and the corresponding duty cycle is the desired duty cycle for the particular irradiation level.

From equation (17), for typical value of R_L, by changing the duty cycle (D) of LUO converter, the load resistance of the PV panel is altered such that always maximum power is extracted from the PV module at any irradiation level and temperature condition. Fig.8 shows that the flowchart of the proposed novel SSB MPPT algorithm with the direct control method in which the duty cycle (d) is calculated directly. P_o and d_O denotes the initial value of PV module power and duty cycle which are taken as 0.5W and 0.5 respectively. The step size of duty cycle (Δd) is taken as 0.02.

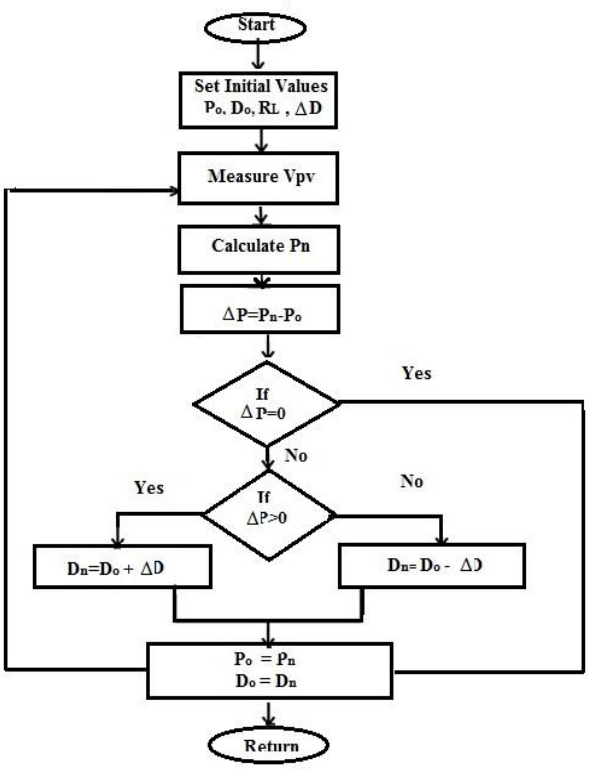

Fig.8 Flow chart of the proposed MPPT algorithm

In proposed SSB algorithm, the maximum power is computed by measuring the PV panel voltage and duty ratio only instead of measuring PV panel voltage and current. For a constant irradiation condition and fixed load resistance, the power versus duty ratio curve is found to be inverted V curve[22] as shown in Fig.9. From this curve, it is clear that power is increased as duty ratio is increased and at one particular duty ratio,it reaches maximum value. The power decreases if the duty ratio is increased beyond this value. Thus by changing duty ratio, it is possible to reach the maximum power. This course of action ultimately moves the effective load line, on the I-V curve of the PV module to a point where maximum power can be extracted.

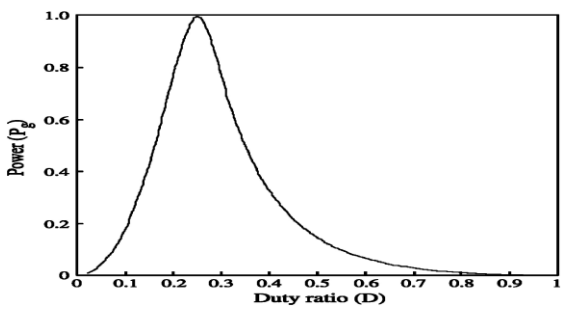

Fig.9 Variation of duty cycle with PV module power

5. Analysis of Simulation Results

The MATLAB simulink model of the proposed stand-alone PV system is developed which consist of the PV module, LUO converter, MPPT controller and a resistive load. Simulation is carried out for existing P&O and proposed SSB algorithms and the results are analysed. Fig.10 shows the simulink model of the proposed system with only voltage sensor used to track the MPP. The LUO converter's parameters are listed in the Table 3.

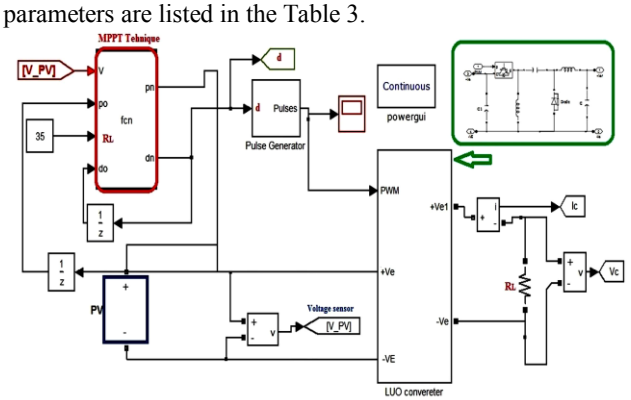

Fig.10 Simulink model of proposed system with only voltage sensor

In order to investigate the proposed MPPT algorithm, constant irradiation level readings and its dynamic behaviors by changing the irradiation level from low to high are taken. The results are verified by compared with existing P&O MPPT method. Fig.11. shows the MPPT tracking features of existing and proposed system, it is observed that initially solar irradiation level is set to 600W/m^2, and then it is increased to 1000 W/m^2 at 0.3sec. As the irradiation level varies, the proposed MPPT controller tracks the new MPP by increase and decrease of duty cycle of converter. Now, the power output of the PV array, which is 24.2W at 600W/m^2 is increased to 39.8W at 1000W/m^2. The voltage of the PV module is increased from 16.9V to 17.4V under that condition. It is also observed that the proposed system works better in terms of fluctuations in the power of the PV module around the MPP, cost and efficiency.

A.Performance evaluation of the proposed system under steady state condition

Steady state response of the proposed PV system is obtained for a constant irradiation of 1000 W/m^2 at t=0sec. Figs. 12(a) & (b).show the simulation results of PV panel output voltage and current for the existing P&O and proposed SSB MPPT technique with macroscopic view for ripple. From the simulation results, it is observed that voltage ripple (ΔV_{PV}) and current ripple (ΔI_{PV}) for the existing MPPT is 2.1V and 29mA respectively, but in proposed MPPT, it is reduced to 1.6V and 0.3mA. Figs.13 (a)&(b) show the converter output voltage and current for the existing P&O and proposed MPPT technique with macroscopic view for ripple. It is observed that voltage ripple (ΔV_O) and current ripple (ΔI_O) for the existing MPPT is 1.9V and 0.4A respectively, in proposed MPPT it is 1.1V and 0.2A only.

B.Performance evaluation of the proposed system under dynamic condition

Dynamic response of the proposed system is studied by varying an irradiation level from 600W/m^2 to 1000W/m^2 after t=0.3sec. Figs 14(a)-(d) show the dynamic response of the PV panel and converter output voltage and current for the existing and proposed SSB algorithms.

From the simulation results, it is observed that proposed system follow as it is existing system and required slight more settling time than the existing system. However, it has more advantage such as simple algorithm, reduced cost due to absence of current sensor, lesser ripple value. The significant ripple reduction is obtained in proposed system, around 25 to 50% reduction in voltage and current ripple as compared to existing method for the various illumination levels.

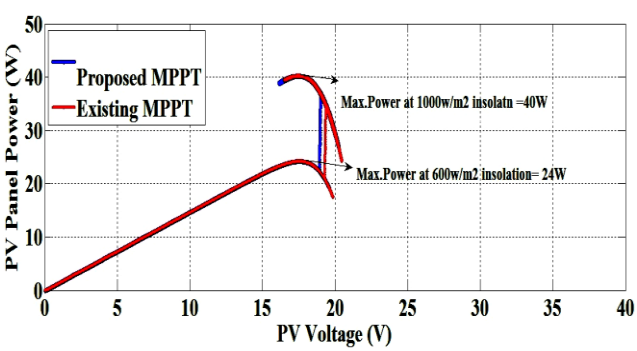

Fig.11 MPPT tracking features of existing and proposed method from 600 to 1000 W/m^2

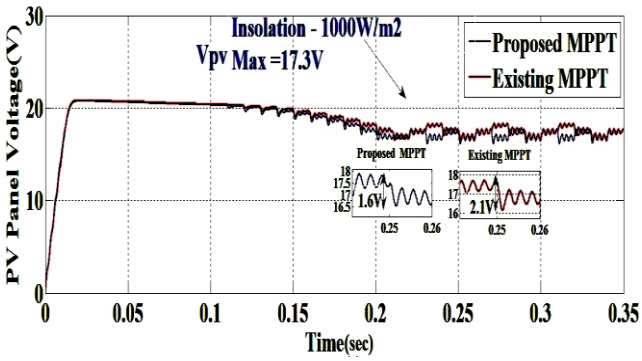

(a)

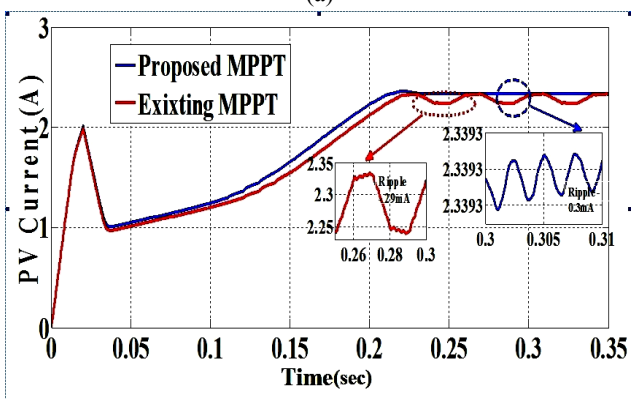

(b)

Fig.12 PV panel output (a) Voltage (b) current - for existing and proposed system at 1000 W/m^2 and its macroscopic view for ripple

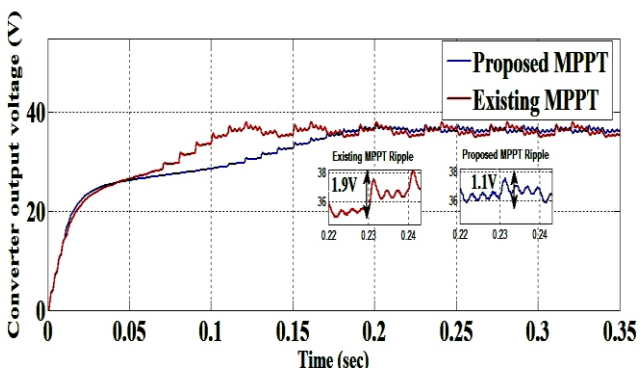

(a)

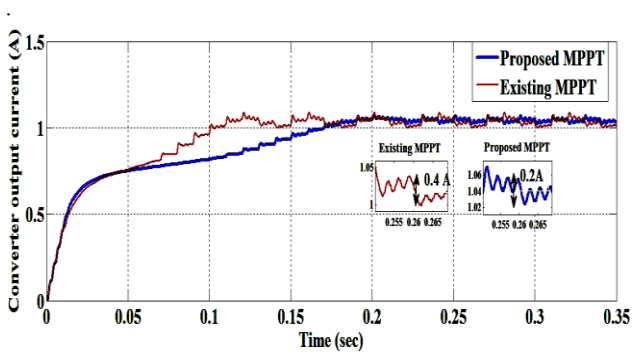

(b)

Fig.13 LUO converter output (a) voltage (b) current - for existing and proposed system at 1000W/m^2 and its macroscopic view for ripple

Table 4 summarizes the PV module and converter output voltage & current ripple amplitude values for the various irradiation levels. According to the obtained results, it is clear that proposed method assured that good ripple reduction under different operating conditions. Fig.15 shows the comparison of efficiency of the power converter in existing and proposed method for varying irradiation conditions.

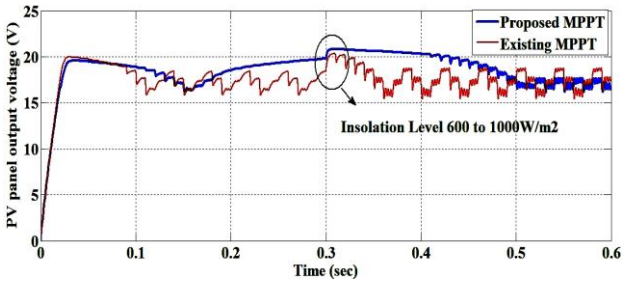

(a)

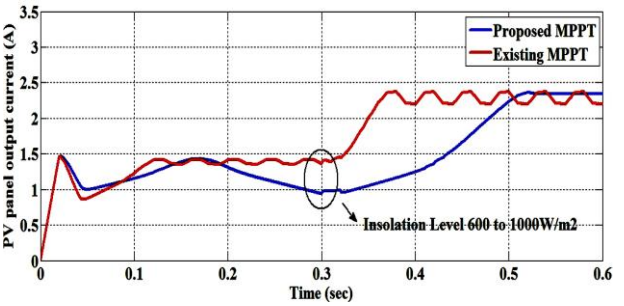

(b)

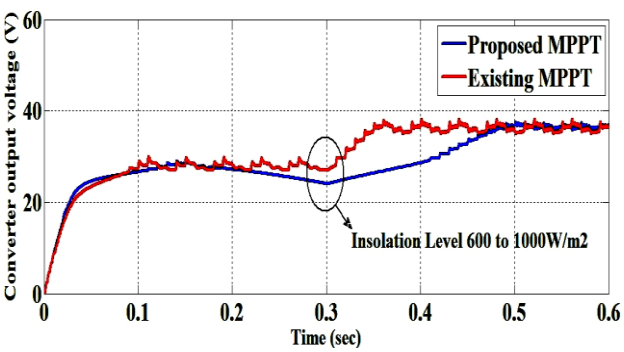

(c)

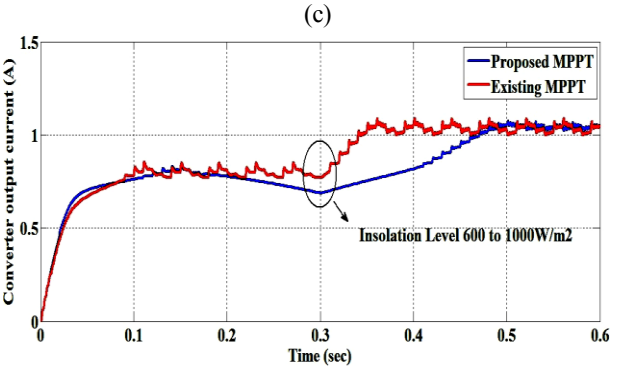

(d)

Fig.14(a) PV panel output voltage for the existing and proposed system (b)PV panel output current for the existing and proposed system.(c) LUO Converter output voltage for existing and proposed system (d)LUO Converter output current for existing and proposed system.

Table 4: Ripple content of the existing P&O and proposed MPPT technique for various irradiation conditions

Irradiation Level (W/m^2)			1000	800	600
Existing P&O MPPT Method	PV Panel	ΔV_{PV}	2.1	2.5	1.5
		ΔI_{PV}	29	90	60
	Converter Output	ΔV_O	1.9	2.1	2.3
		ΔI_O	0.4	0.6	0.6
Proposed SSB MPPT Method	PV Panel	ΔV_{PV}	1.6	1.2	1.1
		ΔI_{PV}	0.3	0.5	0.6
	Converter Output	ΔV_O	1.1	1.3	1.4
		ΔI_O	0.2	0.3	0.3

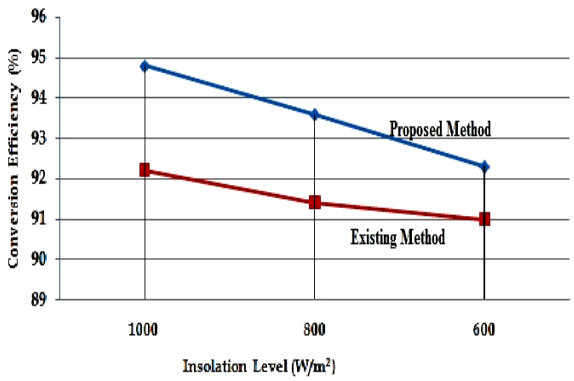

Fig.15 Comparison of conversion efficiency for existing P&O and proposed method for different irradiation level

6. Experimental Result and Discussion

Hardware prototype of LUO converter based stand-alone PV system is built in the laboratory as per the design specification. The system performance is verified at different irradiation conditions. The proposed SSB MPPT control algorithm is implemented using Field Programmable Gate Array (FPGA- Spartan 6 Part No : XC6SLX25-3FTG256). The output of the PV module voltage is sensed and adopted to a scale (<5V) and it is given as analog input to FPGA. The 12 bit binary values of PV voltage samples are obtained from AD7266 (ADC) and it is given to FPGA to generate gate signal for the LUO converter. The software used to develop program is Xilinx and loaded in the FPGA. The synthesis, placement and route are implemented in ISE13.1 environment.

Fig.16 shows the experimental setup for the proposed solar system. The proposed SSB MPPT control algorithm is implemented using Field Programmable Gate Array (FPGA-Spartan 6). Fig.17 shows the gate signal of the switch(S) to the LUO converter at irradiation level is 1000W/m^2.

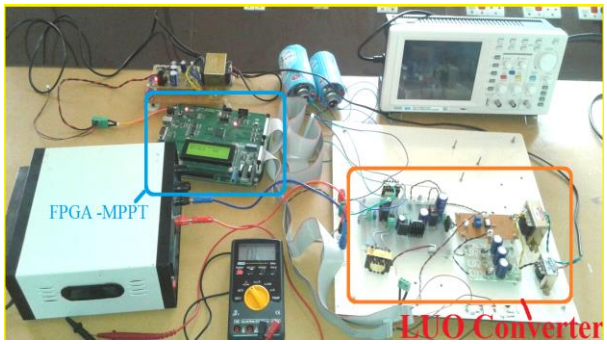

Fig 16 Experimental set up for proposed solar PV system

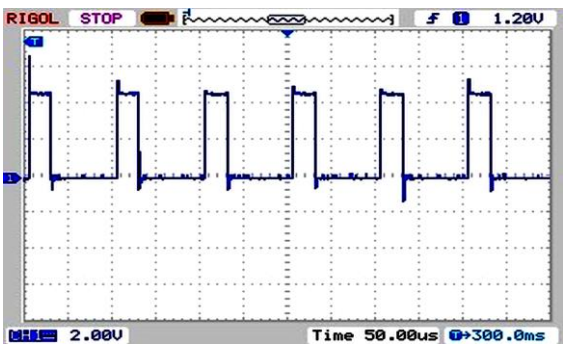

Fig.17 Gate pulse given to the switch (S) in Luo Converter

Fig.18. shows the PV module output voltage for existing and proposed method respectively. It is observed that ripple is reduced in the proposed method considerably 20%. Fig. 19.(a) illustrates the output voltage of LUO converter for the existing and proposed MPPT system and Fig.19.(b) shows the response of the proposed SSB system when irradiation is varied from 1000 W/m^2 to 800 W/m^2. Though both the system have approximately same terminal voltage 36V, the proposed system has less ripple around 3.5% when compared with that of existing P&O method which is 6% at 1000 W/m^2. The results are in close agreement with the simulated results. In addition, the input current is continuous and ripple is minimized as compared to the existing P&O method. The proposed system is cost effective because of usage of single sensor.

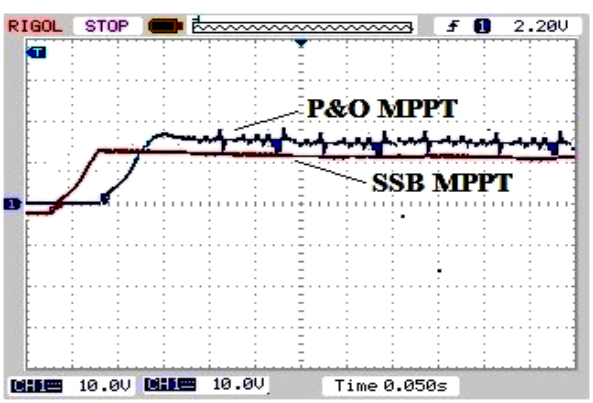

Fig.18 Experimental result of PV panel output voltage for existing P&O and proposed SSB method

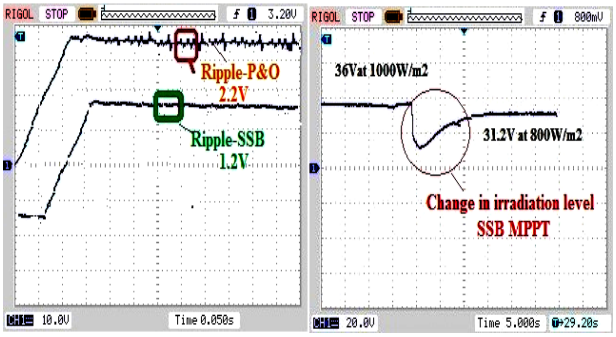

(a) (b)

Fig.19 Experimental result of (a) converter output voltage for existing P&O and proposed SSB method (b)Converter output voltage for proposed system during change in irradiation level.

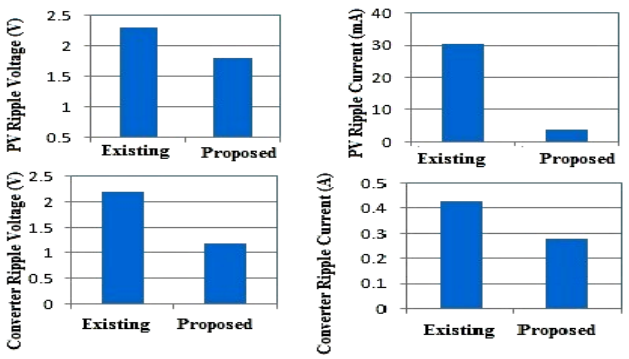

Fig.20 Experimental results of PV and converter side ripple voltage and current comparison for existing and proposed system at 1000W/m^2

To evaluate the performance of the proposed PV system, comparison between existing P&O and proposed SSB MPPT algorithm is carried out for constant illumination level. Fig.20 shows the PV and converter side ripple voltage and current comparison of existing and proposed SSB system at 1000W/m^2. It is observed that the proposed MPPT method have lot of merits when compared to the existing P&O method such as good tracking, less expensive and the complexity of implementing the MPPT algorithm is less. However settling time of the existing system (0.1sec) is slightly lower than the proposed system(0.15sec). An MPPT without current measurement (typical LEM make Hall Effect sensor) can greatly reduce the cost around 18% and is beneficial for small-scale implementation. The Fig.21.shows cost comparison (in terms of sensors) of the existing P&O and proposed SSB MPPT system. Since the current measurement (current sensor) is not required in the proposed SSB system, the realization cost is less. [Cost of voltage and current sensor in Indian rupees around six thousand and two thousand respectively, Source: LEM LV 25-P /LA 55-P, Voltage/Current Transducer].

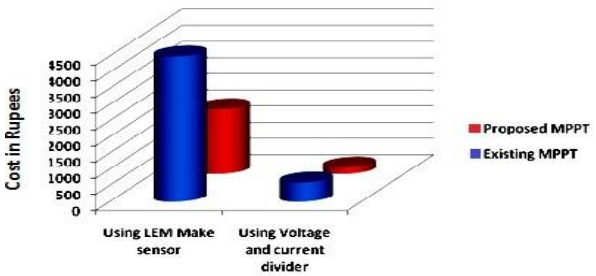

Fig.21 Cost comparison of sensor used in the existing P&O and the proposed SSB MPPT system

7.Conclusion

The single sensor based (Voltage sensor) MPPT algorithm is proposed and implemented using LUO converter for the stand-alone PV system. The results are compared with existing P&O algorithm. A significant drop in voltage and current ripple in PV and load side is observed. The oscillation at MPP is reduced considerably. However, the settling time of the proposed SSB system is slightly higher than that existing P&O based system. The experimental verification of the proposed algorithm is carried out using 40W PV panel. The results confirm the SSB algorithm has higher efficiency, excellent tracking capability and significant reduction in the ripples presents in the PV module and load side. In addition to the system being cost effective.

Acknowledgment

The authors would like to express gratitude to Technical Education Quality Improvement Programme (TEQIP-Under World bank) sponsored Technical institute of Alagappa Chettiar College of Engineering and Technology, Karaikudi, India for giving permission to implement the project in Electrical Engineering Department.

References

1. Mekhilef, R Saidur, and A Safari, "A review on solar energy use in industries," *Renewable and Sustainable Energy Reviews*, vol.15, pp.1777-1790, 2011.
2. W Xiao, F F Edwin, G Spagnuolo, and J Jatskevich, "Efficient Approaches for Modelling and Simulating Photovoltaic Power systems," *IEEE Trans. Photovoltaics*, vol.3, pp.500-508, 2013.
3. D Sera, L Mathe, K S Kerekes, S V Spataru, and R Teodorescu, "ON the Perturb and Observe and Incremental Conductance MPPT methods for PV systems," *IEEE Trans. Photovoltaics*, vol.3, pp.1070-1078, 2013.
4. C H Lin, C H Huang, Y C Du, and J L Chen, "Maximum photovoltaic power tracking for the PV array using the fractional-order incremental conductance method," *Applied Energy*, vol.88, pp.4840–4847, 2011.
5. X Zhi-rong, Z Ping Yang, Dong-bao, L Peng, L Jin-yong, and C Yuan-rui, "An Improved Variable Step Size MPPT Algorithm Based on INC," *Journal of Power Electronics* vol.15, pp. 487-496, 2015.

6. H S H Chung, K K Tse, S Y Ron Hui, C M Mok, and M T Ho, "A novel maximum power point tracking technique for solar panels using a SEPIC or cuk converter", IEEE Transactions on Power Electronics, vol. 18, pp. 717-724, 2003.
7. A Safari, and S Mekhile "Simulation and Hardware Implementation of Incremental Conductance MPPT With Direct Control Method Using Cuk Converter," *IEEE Trans.Industrial Electronics*, vol.58, pp.1154-1161, 2011.
8. S Albert Alexander, T Manikandak, "Digital control strategy for solar photovoltaic fed inverter to improve power quality"' *Journal of Renewable and Sustainable Energy* 6:013128 (1)-(18), 2014.
9. T Esram, and P L Chapman , "Comparison of Photovoltaic Array Maximum Power Point Tracking Techniques," *IEEE Trans.Energy Conversion*, vol.22, pp.439-449, 2007.
10. D M K Schofield , Foster, M P and D.A Stone, "Impact of ripple current on the average output power for solar cells', 6th IET International Conference on Power Electronics", Machines and Drives (PEMD 2012), pp. 1-5 2012.
11. N.D Benavides, and P.L Chapman, "Modeling the effect of voltage ripple on the power output of photovoltaic Modules", IEEE Trans. on Industrial Electronics, vol. 55, no. 7, pp. 2638-2643, 2008.
12. T Esram, I L Illinois Univ Urban, J W Kimball, P T Krein, and Chapman P L, "Dynamic maximum power point tracking of photovoltaic arrays using ripple correlation control," *IEEE Trans. Power Electronics*, vol.21, pp.1282–1291, 2006.
13. S Nema, R K Nema, and G Agnihotri, "Matlab / simulink based study of photovoltaic cells / modules / array and their experimental verification," *International Journal of Energy and Environment*, vol .1, pp.487-500, 2010.
14. S A Rahman, K Rajiv, Varma, and T Vanderheide, "Generalised model of a photovoltaic panel," *IET Renewable Power Generation*, vol.8, pp. 217 – 229, 2013.
15. M H Taghvaee, M A M Radzi, S M Moosavain, HashimHizam and M HamiruceMarhaban, "A current and futurestudy on non-isolated DC–DC converters for photovoltaic applications", Renewable and Sustainable Energy Reviews, vol. 17, pp. 216-227, 2013.
16. S Sivakumar, M JagabarSathik, P S Manoj and G Sundararajan , "An assessment on performance of DC-DC converters for renewable energy applications", Renewable and Sustainable Energy Reviews, vol. 58, pp. 1475-1485, 2016.
17. S Venkatesan and M Saravanan, "Simulation and experimental validation of new MPPT algorithm with direct control method for PV application", Journal of Renewable and Sustainable Energy, vol. 8, no. 4, pp. 043503-043522 2016.
18. F L LUO Hong Ye, "Advanced dc/dc Converters", CRC PRESS, Florida, 2004.
19. S Venkatesan and Saravanan, M , "Modeling and simulation analysis of solar PV energy system with LUO converter using state-space averaging technique", International Journal of Advanced Engineering Technology, vol. 7, no. 2, pp. 770-777, 2016.
20. S Venkatanarayanan and M Saravanan, "Implementation of a Sliding Mode Controller for Single Ended Primary Inductor Converter", Journal of Power Electronics, Vol.15,no.1,pp.39-53 (2015).
21. H S H Chung, K K Tse, S Y Ron Hui, C M Mok, and M T Ho, "A novel maximum power point tracking technique for solar panels using a SEPIC or cuk converter", IEEE Transactions on Power Electronics, vol. 18, pp. 717-724, 2003.
22. M Veerachary, T senjyu and U katsumi, "Voltage-based maximum power point tracking control of PV system", IEEE transactions on aerospace and electronic systems vol. 38, no.1.pp.262-270, 2002.